

# Size- and Shape-Controlled Synthesis of Ferroelectric Plate-like Particles and Their Piezoelectric Characteristics

M. Macek-Krzman<sup>1</sup>, H. Ursic Nemevsek<sup>1</sup>, D. Suvorov<sup>1</sup>, R. Ciobanu<sup>2</sup>

<sup>1</sup>Jožef Stefan Institute, Ljubljana, Slovenia, [marjeta.macek@ijs.si](mailto:marjeta.macek@ijs.si), [hana.ursic@ijs.si](mailto:hana.ursic@ijs.si)

<sup>2</sup>"Gheorghe Asachi" Technical University of Iasi, Iasi, Romania, [rciobanu@tuiasi.ro](mailto:rciobanu@tuiasi.ro)

**Abstract** –  $\text{Ba}_{1-x}\text{Sr}_x\text{TiO}_3$  plate-like particles were prepared by the topochemical transformation of the  $\text{Bi}_4\text{Ti}_3\text{O}_{12}$  template plates in the molten salt. During the conversion, which took place at 900 °C in the presence of high excess of  $\text{BaCO}_3$  and  $\text{SrCO}_3$  ( $\text{Bi}_4\text{Ti}_3\text{O}_{12}$ : ( $\text{BaCO}_3+\text{SrCO}_3$ )=1:10) with the initial Ba:Sr molar ratios equal to 0.98:0.02 and 0.9:0.1, the precursor plate shape was well preserved especially in terms of side length, while the average thicknesses of the final perovskite plates were higher compared to that of template. Energy dispersive spectroscopy (EDS) revealed that the initial Ba:Sr ratio was not maintained during the transformation, namely Sr incorporated more than Ba. The initial Ba:Sr=0.98:0.02 and 0.9:0.1 ratios resulted in the tetragonal  $\text{Ba}_{0.98}\text{Sr}_{0.06}\text{Bi}_{0.02}\text{Ti}_{0.97}\text{O}_3$  and cubic  $\text{Ba}_{0.79}\text{Sr}_{0.24}\text{Bi}_{0.02}\text{Ti}_{0.97}\text{O}_3$  perovskite plates, respectively.

Local Ferroelectric/piezoelectric hysteresis loops that were obtained using a piezoresponse-force microscope (PFM), indicated the significant ferroelectric response of [001] preferentially oriented  $\mu\text{m}$ -sized  $\text{Ba}_{0.98}\text{Sr}_{0.06}\text{Bi}_{0.02}\text{Ti}_{0.97}\text{O}_3$  plates.

**Keywords** – Synthesis, piezoelectric characteristics.

## I. INTRODUCTION

Extremely fast progress in the understanding of physical phenomena, characterization methods and in the development of new materials and devices, creates ever new needs for even better materials, which enables fabrication of smaller, lighter and more efficient devices. Ferroelectric materials are one of those functional materials, which can find very versatile applications as energy harvesters, sensors, actuators, transducers, nonvolatile ferroelectric random-access memories (NVMs) and microwave tunable devices. The direct piezoelectric effect of ferroelectrics can be exploited for electromechanical sensors or energy harvesters, which also enables the development of various self-powered sensors (PH, temperature, velocity, etc.) [1]. The recent

development of several new applications of ferroelectrics in the field of bone regeneration [2], impact detection sensors [3] and energy harvesters on the flexible substrates [4] has increased the interest for the investigations ferroelectric+polymer composites. The majority of these investigations have been done for the mixture of spherical or irregularly shaped ferroelectric particles with the polymers [2, 3]. However, taking into account that the intrinsic piezoelectric effect is not isotropic, what causes larger response along certain crystallographic direction [5, 6], the composites containing defined-shape properly oriented ferroelectric particles are expected to show better piezoelectric performance compared to the spherical particles. For example, it is well known that the crystallographic direction with the maximum piezoelectric response in tetragonal perovskites ( $\text{BaTiO}_3$ ) depend on the  $d_{15}/d_{33}$  ratio. Based on this ratio the ferroelectrics are regarded as rotators or extenders [5, 6]. Extender ferroelectrics exhibit high  $d_{33}$  values and the maximum response along the polar axis. In rotator ferroelectrics with high  $d_{15}$  relative to  $d_{33}$  the maximum longitudinal piezoelectric response is away from the polar axis [5, 6]. Since both of these coefficients are temperature dependent, the extender or rotator characteristics of the material can change with temperature. For example, tetragonal  $\text{BaTiO}_3$  behaves as extender close to the tetragonal to cubic phase transition (380 °K), however when approaching to the low-temperature orthorhombic phase (278 °K)  $\text{BaTiO}_3$  exhibits rotator characteristics, because of high  $d_{15}$  coefficient. Based on this it can be inferred that when designing a piezoelectric device using defined-shape ferroelectric particles, their orientation, the device operation temperature,  $d_{15}$ ,  $d_{33}$  coefficients should be carefully considered. In order to maximize the piezoelectric performance of the ferroelectric-polymer composites, properly oriented defined shape ferroelectric particles are highly required. Chemical substitution represents one of the possibility for tuning of the  $d_{33}$  and  $d_{15}$  coefficients, their ratio and temperature dependence. Ferroelectric defined-shape preferentially oriented

particles, which differ in these characteristics and in their preferential orientation can together with a proper designing cover various application needs in the field of sensors, energy harvesters and in medicine.

In this work we studied the topochemical transformation from  $\text{Bi}_4\text{Ti}_3\text{O}_{12}$  template plates in to  $\text{Ba}_{1-x}\text{Sr}_x\text{TiO}_3$  solid solutions in the molten salt. The research was focused on the synthesis conditions at which, firstly the shape of the initial template was preserved and secondly the  $\text{Ba}_{1-x}\text{Sr}_x\text{TiO}_3$  particles exhibited tetragonal crystal structure. The incorporation ratio of Ba:Sr during the topochemical process was determined. The ferroelectric and piezoelectric properties of the tetragonal perovskite plates were examined by piezoresponse-force microscope (PFM), what have not been reported yet.

## II. EXPERIMENTAL

### A. Preparation of $\text{Bi}_4\text{Ti}_3\text{O}_{12}$ plates

$\text{Bi}_4\text{Ti}_3\text{O}_{12}$  plates were prepared according to the procedure described in [7]. The short summary of the synthesis is as follows:  $\text{Bi}_2\text{O}_3$  nanopowder (Sigma Aldrich 99, 8%) and  $\text{TiO}_2$  (P25, Degussa) were weighed in the stoichiometric ratio of  $\text{Bi}_4\text{Ti}_3\text{O}_{12}$ . The powders were well mixed and ground together with the NaCl and KCl salts, which were added in the amount providing NaCl:KCl: $\text{Bi}_4\text{Ti}_3\text{O}_{12}$ =50:50:1. For the preparation of  $\text{Bi}_4\text{Ti}_3\text{O}_{12}$  plates the mixture was heated to 800°C for 2 hours. The heating and cooling rate was 10 C/min. After the thermal treatment the salt was removed by washing with deionized water. Then the  $\text{Bi}_4\text{Ti}_3\text{O}_{12}$  plates were additionally washed with 3M  $\text{HNO}_3$  for the elimination of  $\text{Na}_{0.5}\text{Bi}_{1.5}\text{ClO}_2$  phase [7]. After additional water washing which was needed for removal of  $\text{HNO}_3$ , the powders were freeze dried.

### B. Preparation of plate-like $\text{Ba}_{1-x}\text{Sr}_x\text{TiO}_3$ plate-like particles

For the topochemical transformation from  $\text{Bi}_4\text{Ti}_3\text{O}_{12}$  template plates in to  $\text{Ba}_{1-x}\text{Sr}_x\text{TiO}_3$  solid solutions the salts and  $\text{BaCO}_3$  were mixed and thoroughly ground and then the  $\text{Bi}_4\text{Ti}_3\text{O}_{12}$  plates were added. All reagents in the molar ratio of KCl:NaCl: $\text{Bi}_4\text{Ti}_3\text{O}_{12}$ :( $\text{BaCO}_3$ + $\text{SrCO}_3$ )=39:39:1:10 were gently homogenised in ethanol to prevent the mechanical damaging of the template plates. Ethanol was evaporated prior the heat treatment, which was done according to the following temperature program: heating 10 C/min to 600°C and 0.5 C/min to 900°C, isothermal annealing for 2 hours at this temperature and cooling 1°C/min to room temperature.  $\text{Ba}_{1-x}\text{Sr}_x\text{TiO}_3$  plate with the initial Ba/Sr ratio of 0.98:0.02 were synthesized by weighing of 2,0 g KCl, 1,56 g NaCl, 0,8 g  $\text{Bi}_4\text{Ti}_3\text{O}_{12}$ , 1,333g  $\text{BaCO}_3$  (Alfa Aesar 99,95%) and 0,0211g  $\text{SrCO}_3$  (Alfa Aesar 99,99%). For the perovskite plates with Ba/Sr initial ratio of 0.9:0.1 the

amount of reagents was the same, except the masses of  $\text{BaCO}_3$  and  $\text{SrCO}_3$  were 1,2242 g and 0,1017 g, respectively. The syntheses were performed in the round  $\text{Al}_2\text{O}_3$  crucibles with diameter of 5 cm. After the reaction the salt was removed by washing with distilled water. The large black particles, which composition was previously determined to be  $\text{BaBiO}_3$  [7], were removed by sedimentation, while the other side products were eliminated by washing with  $\text{HNO}_3$  (2M  $\text{HNO}_3$ ). Finally, the  $\text{Ba}_{1-x}\text{Sr}_x\text{TiO}_3$  plates were washed with water and ethanol and then dried in air. The detailed washing procedure is given in [7].

### C. Characterization

The crystal structure of the samples was analysed using a D4 Endeavor (Bruker AXS, Karlsruhe, Germany) X-ray diffractometer using Cu-K $\alpha$  radiation (1.5406 Å).

The particles were examined using a field-emission scanning electron microscope (FE-SEM, JSM-7600 F, JEOL) equipped with an Oxford Instruments Inca energy-dispersive X-ray spectrometer (EDS). For the EDS analysis the  $\text{Ba}_{1-x}\text{Sr}_x\text{TiO}_3$  particles were deposited on the polished graphite substrate and coated with carbon (12 nm) to prevent charging. At least 7 measurements on different  $\text{Ba}_{1-x}\text{Sr}_x\text{TiO}_3$  plates were performed for each examined composition.

The particle sizes (side length (L) and thickness (d)) were evaluated from the SEM images with the help of Smile View software (JEOL, Tokyo, Japan). For the statistics of the side length distribution 200–300 particles were assessed. Due to the plate shape of the majority of the particles, fewer plates were lying perpendicular to the substrate and thus the average thicknesses (d) were merely estimated from 10–80 particles.

For the estimation of the preferential growth orientation of the  $\text{Ba}_{1-x}\text{Sr}_x\text{TiO}_3$  plates, a few drops of the suspension of coated plates in butanol were deposited on a Si-single crystal. The majority of the plates deposited, using this method, were lying flat, with their larger surface on the Si-single crystal. For the coating of the  $\text{Ba}_{1-x}\text{Sr}_x\text{TiO}_3$  particles, 2 ml of octadecyldimethyl(3-trimethoxysilylpropyl)ammonium chloride ( $\text{C}_{26}\text{H}_{58}\text{ClNO}_3\text{Si}$  (SILAN)) (40 % in methanol) was added to the water suspension of  $\text{Ba}_{1-x}\text{Sr}_x\text{TiO}_3$  plates (50 mg/25 ml). The agglomerates of plates were broken by means of ultrasound. The excess of SILAN was removed by water washing. The particles were separated from the water by centrifugation. The remains of water were washed out with n-butanol. Finally, the plates were dispersed in n-butanol by means of ultrasound. The efficiency of deagglomeration was checked by examination of dried drop of suspension by SEM and XRD.

The piezoelectric and ferroelectric characteristics of the  $\text{Ba}_{1-x}\text{Sr}_x\text{TiO}_3$  plates were examined PFM. In order to avoid the  $\text{Ba}_{1-x}\text{Sr}_x\text{TiO}_3$  plates sticking to the PFM tip, the  $\text{Ba}_{1-x}\text{Sr}_x\text{TiO}_3$  plates were fixed on the  $\text{SrTiO}_3$  substrate

using a thermal treatment (heating to 700°C). We selected non-conductive SrTiO<sub>3</sub> substrate in order to avoid electrical breakdown through the air, which could be a problem when measuring the small, micrometre-sized plates on a large conductive substrate.

The topography (height image, contact mode) and the PFM images were recorded with an atomic force microscope (AFM; Asylum Research, Molecular Force Probe 3D, Santa Barbara, CA) equipped with a Dual AC Resonance Tracking (DART) Switching Spectroscopy (SS) mode. A Ti/Ir-coated Si tip with a radius of curvature ~20 nm (Asyelec, AtomicForce F&E GmbH, Mannheim, Germany) was used. The out-of-plane PFM images were measured in the DART mode (at 4 V and frequency 369 kHz), the local hysteresis loops were measured in the SS mode with the waveform parameters: increasing step signal with maximum amplitude of 60 V and frequency 0.2 Hz; overlapping sinusoidal signal of amplitude 4 V and frequency 20 Hz, off-loop mode (2 cycles).

The Curie temperature (T<sub>c</sub>) and the enthalpy of the ferroelectric-paraelectric phase transition was determined using a Mettler Toledo DSC1 STARe System.

### III. RESULTS AND DISCUSSION

In our previous work [7] we studied the topochemical transformation from Bi<sub>4</sub>Ti<sub>3</sub>O<sub>12</sub> in to BaTiO<sub>3</sub>. With respect to the complete solid solubility between BaTiO<sub>3</sub> and SrTiO<sub>3</sub>, we expected that Ba<sub>1-x</sub>Sr<sub>x</sub>TiO<sub>3</sub> plates may also form via similar mechanism. We decided to study this transformation because partial substitution of Ba with Sr represents the possibility for tuning the ferroelectric characteristics of the perovskite plates.

Like in our previous research [7] the synthesis of Bi<sub>4</sub>Ti<sub>3</sub>O<sub>12</sub> template in molten salt at 800°C for 2 hours resulted in μm-sized plate-like particles (Fig. 1a) with orthorhombic crystal structure (PDF:04-016-3435) and 001 preferential orientation (Fig. 2, curve a). The average side length was slightly larger than that in the reported article [7]. Taking into account that the Ba<sub>1-x</sub>Sr<sub>x</sub>TiO<sub>3</sub> solid solubility exists in the whole concentration range between BaTiO<sub>3</sub> and SrTiO<sub>3</sub>, it was expected that the topochemical transformation from Bi<sub>4</sub>Ti<sub>3</sub>O<sub>12</sub> into Ba<sub>1-x</sub>Sr<sub>x</sub>TiO<sub>3</sub> plates may occur via similar mechanisms as that reported for BaTiO<sub>3</sub> [7]. For this reason we use the same initial ratio of the reagents (KCl:NaCl:Bi<sub>4</sub>Ti<sub>3</sub>O<sub>12</sub>:(BaCO<sub>3</sub> + SrCO<sub>3</sub>) = 39:39:1:10) as in our previous work. The initial molar ratio of BaCO<sub>3</sub>:SrCO<sub>3</sub> was set to 0.98:0.02 and 0.9:0.1 which was expected to result into Ba<sub>0.98</sub>Sr<sub>0.02</sub>TiO<sub>3</sub> and Ba<sub>0.9</sub>Sr<sub>0.1</sub>TiO<sub>3</sub>, under the assumption that Ba:Sr ratio during conversion did not change. According to calculations and experiments tetragonal crystal structure was anticipated for the both compositions [8]. However, the XRD examination of the single phase reaction

products after the acid-washing showed that only the composition with the initial Ba:Sr ratio of 0.98:0.02 exhibited tetragonal crystal structure, while no splitting of the (100) diffraction lines in the XRD pattern of the composition with the initial Ba:Sr=0.9:0.1 indicated cubic crystal structure (Fig.2, curves b and c). Since no secondary phases were noticed neither in the XRD patterns nor in the SEM micrographs (Fig. 1 b and c), we assume that Sr similar to Ba react with Bi<sub>2</sub>O<sub>3</sub> forming similar secondary phases which were removable by acid washing (2M HNO<sub>3</sub>) [7]. It can be seen from Fig. 1 and Table 1, that for both compositions the plate shape of the Bi<sub>4</sub>Ti<sub>3</sub>O<sub>12</sub> was well preserved in terms of side length (L), while their thicknesses (d) were higher. The average thickness of the plates with the initial Ba:Sr=0.9:0.1 ratio was slightly smaller compared to that of the plates with higher Ba content. More compositions should be examined in order to verify whether this is related to the composition.

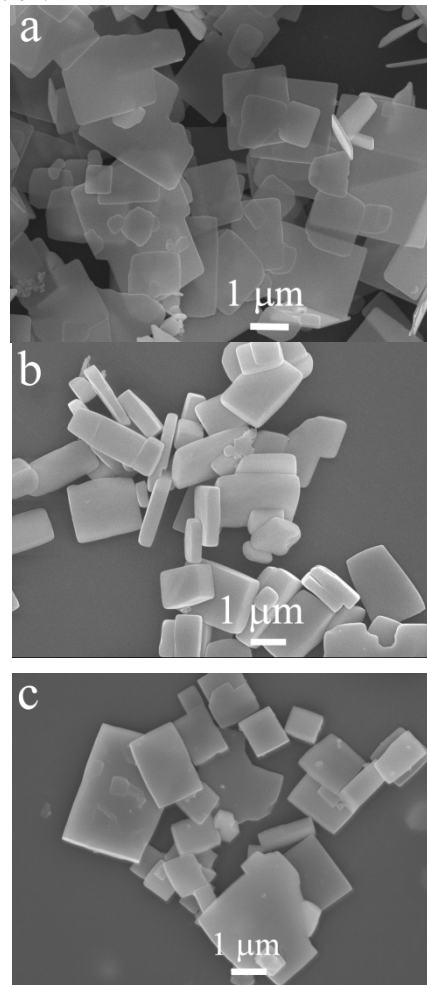


Fig. 1. SEM micrographs of Bi<sub>4</sub>Ti<sub>3</sub>O<sub>12</sub> plates (a) and Ba<sub>1-x</sub>Sr<sub>x</sub>TiO<sub>3</sub> plates with the initial Ba:Sr ratio of 0.98:0.02 (b) and 0.9:0.1 (c)

The cubic crystal structure of the Ba<sub>1-x</sub>Sr<sub>x</sub>TiO<sub>3</sub> with the initial Ba:Sr ratio of 0.9/0.1 was explained by the

EDS analysis, which revealed that Sr incorporate in higher amount than expected. The normalized compo-

Table 1. Average side lengths ( $L$ ), thicknesses ( $d$ ) and compositions of  $Ba_{1-x}Sr_xTiO_3$  plates prepared by the topochemical conversion of  $Bi_4Ti_3O_{12}$  template plates

	Initial Ba:Sr ratio	$L$ ( $\mu\text{m}$ ) (S.D.)	$d$ ( $\mu\text{m}$ ) (S.D.)	Normalized composition determined by EDS
$Bi_4Ti_3O_{12}$ template plates $L=1.9 \mu\text{m}$ (S.D.:1.2) $d=70 \text{ nm}$	0.98:0.02	1,6 (0.7)	0.4 (0.15)	$Ba_{0.98}Sr_{0.06}Bi_{0.02}Ti_{0.97}O_3$
	0.9:0.1	1,9 (1,0)	0.3 (0.1)	$Ba_{0.79}Sr_{0.24}Bi_{0.02}Ti_{0.97}O_3$

sition obtained by the EDS was  $Ba_{0.79}Sr_{0.24}Bi_{0.02}Ti_{0.97}O_3$  (Table 1). According to the literature data the solid solution with such amount of Sr is expected to have  $T_c$  close to the room temperature [8]. Similarly, the higher incorporation of Sr was observed also for the composition with the initial Ba:Sr ratio of 0.98:0.02. Both EDS results also showed some small amount of Bi was also present. Since their concentration was less than 0.5 at. %, this amount was not expected to deteriorate the properties. It can be also inferred from these EDS results that the ratio between the cations, which could occupy the A site ( $Bi^{3+}$ ,  $Ba^{2+}$ , and  $Sr^{2+}$ ) and  $Ti^{4+}$  on the B site is larger than 1, what imply the formation of Ti vacancies. However, other characterization technique should be included to verify this.

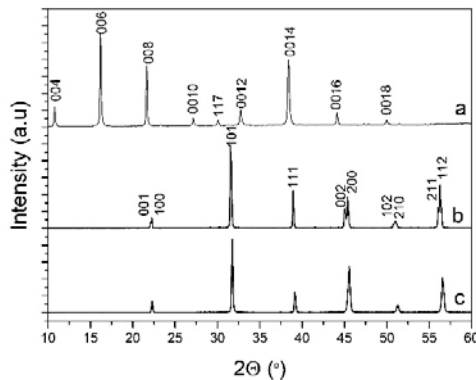


Fig. 2. XRD patterns of  $Bi_4Ti_3O_{12}$  plates cast on the Si-single crystal (a) and  $Ba_{1-x}Sr_xTiO_3$  powders with the initial Ba:Sr ratio of 0.98:0.02 (b) and 0.9:0.1 (c).

According to the  $Ba_{0.98}Sr_{0.06}Bi_{0.02}Ti_{0.97}O_3$  composition, which was determined by the EDS in the case of initial Ba:Sr ratio 0.98:0.02, the  $T_c$  was expected to be between 106 and 116 °C [8]. DSC investigations showed the endothermic peak around 113°C, what is close to the predicted value. The phase transition enthalpy of 0,28 J/g was smaller compared to that reported for the sintered ferroelectric  $BaTiO_3$  ceramics (0.9 J/g) [9]. Based on the fact that the enthalpy value of the ferroelectric phase transition is not determined only by the polarization, but also by the domain structure and strains, the lower enthalpy value was anticipated.

Namely, in the  $BaTiO_3$  plates the domains are not so clamped as in sintered ceramics.

In the XRD pattern of the  $Ba_{1-x}Sr_xTiO_3$  plates with the initial Ba/Ti =0.98:0.02 cast on the Si-single crystal the diffraction lines with the highest intensities were those produced by the (001), (100), (002) and (200), while (101), (110) and (111) diffraction lines were nearly not visible (Fig. 4). Similar as for  $BaTiO_3$  plates, the typical (001)/(100) peak splitting indicated the presence of *a*-((100) orientation (in-plane)) and *c*- ((001) orientation (out of plane)) domains in the substituted  $Ba_{0.98}Sr_{0.06}Bi_{0.02}Ti_{0.97}O_3$  plates.

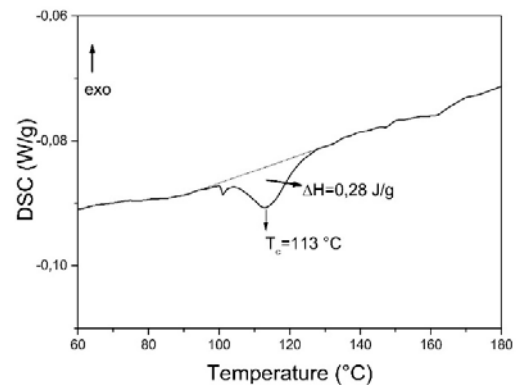


Fig. 3. DSC curve for  $Ba_{1-x}Sr_xTiO_3$  plates with the initial Ba/Sr ratio of 0.98:0.02.

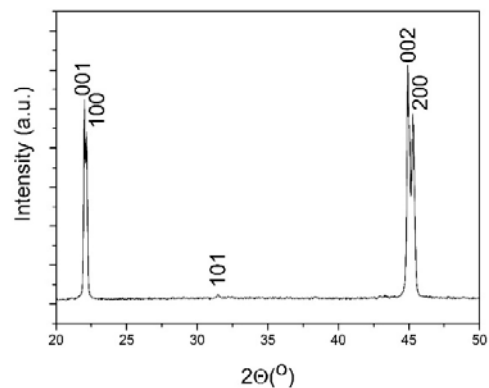


Fig. 4. XRD pattern of  $Ba_{1-x}Sr_xTiO_3$  plates with the initial Ba/Sr ratio of 0.98:0.02 cast on the Si-single crystal (agglomeration of the plates was prevented with coating of the particles with  $C_{26}H_{58}ClNO_3Si$  (SILAN))

The domain nature of the plates was attempted to be examined by the PFM measurements. Since during preparation of the plate suspension in iso-propanol the agglomerates of the plates were not broken into singular plates, typically several particles were sticking together. For this reasons it was not possible to distinguish between the domains in a single particle and the bunch of particles.

However, some features (example is marked with an arrow in Fig. 5.b resemble irregular domains previously observed in BaTiO<sub>3</sub> plates [7] and also in other materials [10]. Furthermore, based on the enhancement of the PFM signal (bright regions in Fig. 5.b it is evident that the Ba<sub>0.98</sub>Sr<sub>0.06</sub>Bi<sub>0.02</sub>Ti<sub>0.97</sub>O<sub>3</sub> plates (initial Ba:Sr=0.98:0.02) exhibited piezoelectric behaviour. This was confirmed also by the PFM switching spectroscopy experiment, which revealed the local hysteresis loops typical for ferroelectrics, Fig. 5.c.

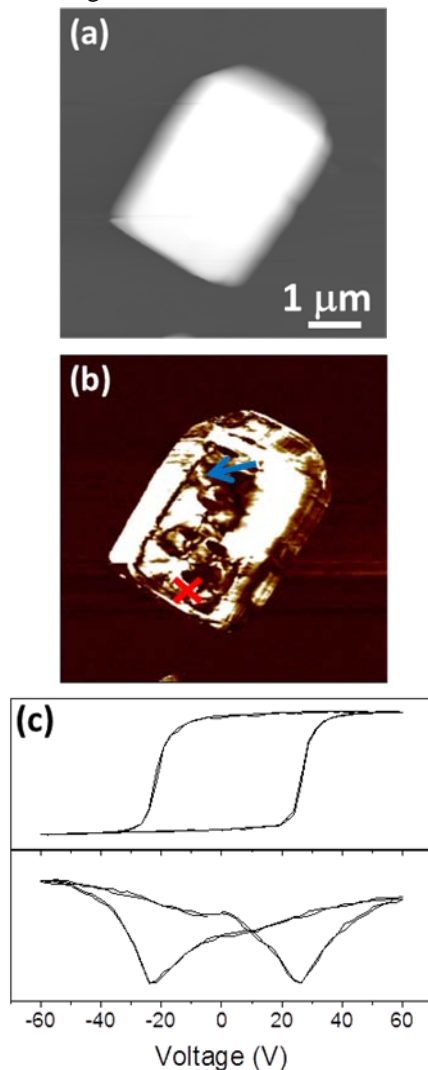


Fig. 5. Topography (a), PFM out-of-plane amplitude image (b) and local hysteresis loops (c); amplitude (below) and phase (above)

The complete dispersion of the ferroelectric plates in the alcohol could be obtained by coating of the plates with the organic molecules, which represent the steric hindrance and prevent agglomeration. In our case the Ba<sub>0.98</sub>Sr<sub>0.06</sub>Bi<sub>0.02</sub>Ti<sub>0.97</sub>O<sub>3</sub> plates (initial Ba:Sr=0.98:0.02) were coated with octadecyldimethyl(3-trimethoxysilylpropyl)ammonium chloride (C<sub>26</sub>H<sub>58</sub>ClNO<sub>3</sub>Si (SILAN)) surfactant and dispersed in butanol. The complete breaking of the agglomerates was confirmed by SEM investigations and it is also evident from the XRD pattern of such plates on the Si-single crystal (Fig. 4). Randomly oriented plates in the agglomerates are expected to contribute to the higher intensities of the (101) and (111) diffraction lines. These were not visible in the XRD pattern of the SILAN-coated Ba<sub>0.98</sub>Sr<sub>0.06</sub>Bi<sub>0.02</sub>Ti<sub>0.97</sub>O<sub>3</sub> plates (initial Ba:Sr=0.98:0.02), what indicated that all plates were well separated lying flat with their largest surface on the Si-single crystal substrate (Fig. 4). Due to the presence of Si in the SILAN molecule annealing to 700°C, which was needed for fixation of the particles for PFM measurements, do not provide complete elimination of the surfactant molecule. The other surfactant, which exhibit similar deagglomeration efficiency as SILAN, will be searched and the examination of the domain structure of individual plates by the PFM is planned to be done in the near future.

#### IV. CONCLUSIONS

Topochemical transformation from Bi<sub>4</sub>Ti<sub>3</sub>O<sub>12</sub> in to Ba<sub>1-x</sub>Sr<sub>x</sub>TiO<sub>3</sub> plates in the molten salt was found to be appropriate method for preparation of highly oriented perovskite plates. The initial Ba:Sr ratio was not preserved during the conversion, because Sr incorporated in the plates more than Ba. In accordance with the Sr content formed Ba<sub>0.98</sub>Sr<sub>0.06</sub>Bi<sub>0.02</sub>Ti<sub>0.97</sub>O<sub>3</sub> and Ba<sub>0.79</sub>Sr<sub>0.24</sub>Bi<sub>0.02</sub>Ti<sub>0.97</sub>O<sub>3</sub> perovskite plates exhibited tetragonal and cubic crystal structure, respectively.

Preferentially [001]-oriented tetragonal Ba<sub>0.98</sub>Sr<sub>0.06</sub>Bi<sub>0.02</sub>Ti<sub>0.97</sub>O<sub>3</sub> plates exhibited good ferroelectric and piezoelectric properties, as determined by PFM.

#### V. ACKNOWLEDGMENT

The present research was performed in the scope of 3184 HarvEnPiez project (Innovative nano-materials and architectures for integrated piezoelectric energy harvesting applications). The research team would like to acknowledge the project M-era.Net Initiative for the funds that supported the HarvEnPiez project. The authors would also like to thank to prof. dr. Romana Cerc Korošec for performing the DSC measurements and to Martina Štefko for her help in the preparation of samples.

#### REFERENCES

- [1] Alluri et al., *ACS Appl. Mater. Interfaces*, 7 (2015) 9831-9840
- [2] Zhang et al, *ACS Nano*, 10 (2016) 7279-7286.
- [3] Capsal et al., *Smart Materials and Structures*, 21 (2012) 055021 1-7.
- [4] Gao et al., *J. Mater. Chem A* 3 (2015) 9965-9971.
- [5] Damjanovic et al., *Appl. Phys Lett* 80 (2002) 652-654.
- [6] Davis et al., *J. Appl. Phys.* 101 (2007) 054112 1-10.
- [7] Kržmanc et al , *Cryst. Growth &Des* 17 (2017) 3210-3220.
- [8] Dawson et al, *Chem. Mater.*, 26 (2014) 6104-6112.
- [9] Kržmanc et al., *Ceram. Int.*, 41(2015) 15128-15137.
- Ursic et al., *J Phys. D Appl Phys.*, 49 (2016) 115304 1-4.